The finite element method for simulations of magnetically driven flows

K. Fraňa and J. Stiller

Abstract— The magnetically induced flow was examined numerically using a computational code based on the finite element method with the streamline-upwind/pressure-stabilized Petrov-Galerkin approach. The mathematical model considers an incompressible isothermal unsteady flow with a low frequency and low induction magnetic field. The validation of the magnetic force calculation was carried out on a cylindrical cavity, where the time-dependent electric potential and current density distribution can be derived analytically. The flow under the rotating magnetic field was simulated for the axisymmetric cylindrical and non-axisymmetric square cavity. The effect of the different geometries on the distribution of the time-averaged magnetic force and magnetically driven rotating flow were discussed.

Keywords— Finite element methods, magnetic forces, rotating flows, stabilization techniques.

I. Introduction

Various kinds of magnetic fields such as rotating (RMF) or traveling magnetic field (TMF) are successfully applied in metallurgical and single crystal growth processes [10]. In order to use these techniques effectively, an in-depth knowledge about the effects of the magnetic field on electrically conducting fluids is needed. The fact, that experimental approaches are mainly too expensive for such investigations then a numerical simulation was found to be an attractive way for extensive magnetically driven flow studies. An overview of results achieved mainly by numerical simulations can be found e.g. in [2],[3],[5],[9], and [13].

The paper is organized as follows: in Section 2, the mathematical model is introduced. The numerical approaches dealing with the finite-element discretization and stabilization techniques are illuminated. Section 3 reports on the code validation. The consequence of the axisymmetric and non-axisymmetric shape of the container on the flows is presented and is discussed in Section 4.

II. Problem formulations

The container, bound by electrically insulated walls the

characteristic length L and the height H, is filled by an electrically conducting fluid with the density ρ, kinematical viscosity ν and electrical conductivity σ. The fluid inside is stirred by the rotating magnetic field with a magnetic induction **B** and frequency ω. The incompressible viscous flow is governed by the Navier-Stokes equation and the continuity equation taking a form as

$$\frac{\partial \mathbf{u}}{\partial t} + \nabla \cdot \mathbf{uu} = -\nabla p + \nabla^2 \mathbf{u} + \mathbf{f} \tag{1}$$

$$\nabla \cdot \mathbf{u} = 0 \tag{2}$$

with Dirichlet and Neumann type boundary conditions

$$\mathbf{u} = \mathbf{g} \tag{3}$$

$$\mathbf{n} \cdot (p + \nu \nabla^2 \mathbf{u}) = \mathbf{h} \tag{4}$$

where the velocity **u** and time t are scaled by ν/L, L^2/ν, the pressure p by $\rho\nu^2/L^2$ and an external mean body force **f** is scaled by $\rho\nu^2/L^3$.

For the calculation of the magnetic body force, the low-frequency and the low-induction RMF condition are assumed. To satisfy these conditions, the magnetic Reynolds number Rm and the shielding parameter S have to be in relation to that of $Rm = \mu\sigma u R << S = \mu\sigma\omega R \leq 1$, where μ denotes the magnetic permeability. Using Ohm's law, the current density is in

$$\mathbf{f} = 2Ta(\mathbf{j} \times \mathbf{B}) = 2Ta(-\nabla\Phi - \frac{\partial \mathbf{A}}{\partial t} + \mathbf{u} \times \mathbf{B}) \times \mathbf{B} \tag{5}$$

where Φ and A denote the dimensionless electric potential and the vector potential, and **j** is the dimensionless current density. The Taylor number is defined as follows:

$$Ta = \frac{\sigma\omega B_0^2 L^4}{2\rho\nu^2} \tag{6}$$

where B_0 is an amplitude of the magnetic field induction and L is the characteristic length. The characteristic length is either the radius of the container R (cylindrical cavity) or half the side length A (square container).

To determine the electric potential Φ in (5), we can exploit that $\nabla \cdot \mathbf{j} = 0$ and at boundaries $\mathbf{j} \cdot \mathbf{n} = 0$. Thus, the equation

K. Fraňa, the Department of Power Engineering Equipment, the Technical University of Liberec, Studentska 2, 461 17 Liberec, Czech Republic, (phone: +420 485 353 436, fax: +420 485 353 644, e-mail: karel.frana@seznam.cz, http://orion.kez.tul.cz/frana)

J. Stiller, the Institute of Aerospace Engineeing, Dresden University of Technology, D-01062, Dresden, Germany, (e-mail: joerg.stiller@tu-dresden.de)

for electric potential derived on the basis of Ohm's law is in this form

$$\nabla^2 \cdot \Phi = -\nabla \cdot \left[\frac{\partial \mathbf{A}}{\partial t} - (\mathbf{u} \times \mathbf{B}) \right] = 0 \tag{7}$$

with the Neumann type boundary condition

$$\frac{\partial \Phi}{\partial n} = -\frac{\partial A_n}{\partial t} \tag{8}$$

For the infinite-length container, $\partial \Phi / \partial n = 0$, otherwise $\partial \Phi / \partial n = -\partial A_n / \partial t$.

Practically, the time-dependent Lorentz force distribution is computed using (5), (7), and (8). Nevertheless, this body force can be divided further into two parts; the time-dependent and the mean part, respectively.

Under considerations that the interaction parameter is $N = \sigma B^2 / \rho \omega \ll 1$ only the mean part of the magnetic body force has a significant effect on the magnetically induced fluid flow and the fluctuating part can be neglected [7] and [8]. Thus, the mean part of the magnetic body force is calculated and averaged in the frame of the one time step instead of the time-consuming calculation in every time step. To find details about the averaging of the magnetic force in respect to the accuracy we refer to [6].

III. NUMERICAL APPROACHES

The finite element discretization space of Ω with boundary Γ is consisted of Ω_e, where e=1,2,...,n_{el} and n_{el} is the number of elements. For velocity and pressure, we define the finite element trial function space denoted as S_u^h and S_p^h, and weighting function υ_u^h and υ_p^h. These function space are selected for H1$_h(\Omega)$, where H1$_h(\Omega)$ is the finite-dimension function space over Ω. Equation (1) and (2) can be formally integrated in time and is written as follows: find $\mathbf{u}^h \in S_u^h$ and $p^h \in S_p^h$ such that $\forall \mathbf{w}^h \in \upsilon_u^h$, $\forall q^h \in \upsilon_p^h$

$$\int_\Omega \mathbf{w}^h \left(\frac{\mathbf{u}^{n+1} - \mathbf{u}^n}{\Delta t} + \nabla \cdot \overline{\mathbf{u}}\overline{\mathbf{u}} + -\overline{\mathbf{f}} + \nabla \overline{p} \right) d\Omega$$

$$+ \int_\Omega \left(\nabla \mathbf{w}^h \right)^T : \nabla \overline{\mathbf{u}}\, d\Omega - \int_\Gamma \mathbf{w} \cdot \partial_n \overline{\mathbf{u}}\, d\Gamma + \int_\Omega q^h \nabla \cdot \mathbf{u}^{n+1}\, d\Omega$$

$$+ \sum_{e=1}^{n_{el}} \int_{\Omega^e} \left(\tau_{SUPG}\, \overline{\mathbf{u}} \cdot \nabla \mathbf{w}^h \right) \cdot (\overline{\mathbf{r}})\, d\Omega$$

$$+ \sum_{e=1}^{n_{el}} \int_{\Omega^e} \left(\tau_{PSPG}\, \nabla q^h \right) \cdot (\overline{\mathbf{r}}) = 0. \tag{9}$$

where the residual $\overline{r}$ is defined as

$$\overline{\mathbf{r}} = \partial_t \overline{\mathbf{u}} + \nabla \cdot \overline{\mathbf{u}}\overline{\mathbf{u}} - \overline{\mathbf{f}} - \nabla^2 \overline{\mathbf{u}} + \nabla \overline{p}. \tag{10}$$

The overbar denotes the time averaged over the time interval given by t_n and t_{n+1}. To the standard Galerking formulation of (1) and (2); the SUPG (streamline-upwind/Petrov-Galerkin) and PSPG (pressure-stabilizing/Petrov-Galerkin) terms are added. An appropriate choice for τ_{SUPG} and τ_{PSPG} is given by [12] and [11]. Both stabilization terms represent weighted residuals, and therefore maintain the consistency of the formulation

The magnetic body force can be trivially calculated if the current density field is known. The right side of (5) is applied for the calculation of the current density field and it is integrated as follows: find $\mathbf{j}^h \in S_j^h$ such that $\forall \mathbf{w}^h \in \upsilon_j^h$, where S_j^h represents the finite element trial function space and υ_j^h weighting function

$$\int_\Omega \mathbf{w}^h \left[\mathbf{j} + \nabla \Phi + \frac{\partial \mathbf{A}}{\partial t} - (\mathbf{u} \times \mathbf{B}) \right] d\Omega + \int_\Gamma \mathbf{w}^h\, \partial_n \mathbf{j}\, d\Gamma = 0. \tag{11}$$

The boundary integral is zero because of $\mathbf{j} \cdot \mathbf{n} = 0$. The time derivation of the vector potential is known for a particular type of the magnetic field. The electric potential must be calculated based on (7), and after integration takes the form: find $\Phi^h \in S_\Phi^h$ such that $\forall q^h \in \upsilon_\Phi^h$, where S_Φ^h represents the finite element trial function space and υ_Φ^h weighting function

$$\int_\Omega \nabla q^h \cdot \left[\nabla \Phi + \frac{\partial \mathbf{A}}{\partial t} - (\mathbf{u} \times \mathbf{B}) \right] d\Omega$$

$$+ \int_\Gamma q^h \partial_n \left[-\nabla \Phi - \frac{\partial \mathbf{A}}{\partial t} + (\mathbf{u} \times \mathbf{B}) \right] d\Gamma = 0 \tag{12}$$

In this equation, the boundary integral vanishes because of the Neumann type boundary for the electric potential (8).

The integrated Equation (9) is further split into a velocity (predictor) and a pressure (corrector) step. The predictor step for velocity is solved explicitly using the Jacobi iterative method, the corrector step involving the pressure equation is solved implicitly by the Conjugated gradient method. The equation (11) and (12) are solved iteratively by the Jacobi method.

For the time averages, the second-order Adams-Bashforth method is applied. The calculation of the mathematical model is fully parallelized. The created computational grid is

decomposed into a specific number of partitions using the *METIS* package [1] (see Figure 1).
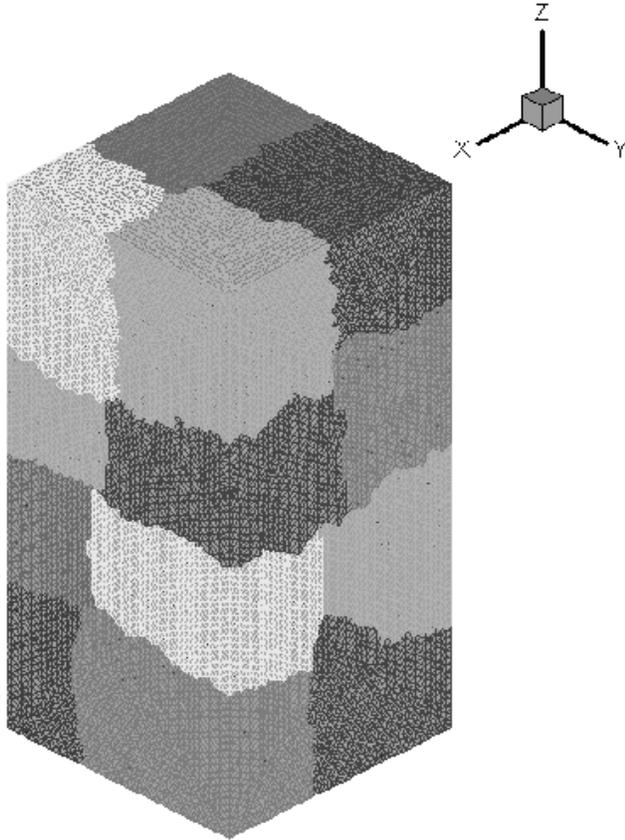
$$\Phi = \sum_{n=1}^{\infty} c_n J_1(\lambda_n r) \sinh(\lambda_n z) \qquad (13)$$

Where J_1 is the Bessel function of the first kind and and λ_n is the zeros of their first derivative, respectively. The function c_n is defined as follows:

$$c_n = \frac{2}{\lambda_n(\lambda_n^2 - 1)J_1(\lambda_n)\cosh(\lambda_n h)} \qquad (14)$$

The analytical expression of the equation for calculation of the current density components e.g. in the y-component is taking the form

$$j_y = \sum_{n=1}^{\infty} c_n \lambda_n \frac{J_0(\lambda_n r) - J_2(\lambda_n r)}{2} \sinh(\lambda_n z) \qquad (15)$$

and in the z-component

$$j_z = r - \sum_{n=1}^{\infty} c_n \lambda_n J_1(\lambda_n r) \cosh(\lambda_n z). \qquad (16)$$

Fig.1 computational grid decomposed into 16 grid partitions

For handling of computational grids, the MG grid library [4] was used which provides a data structure and basic procedures.

IV. CODE VALIDATIONS

The code validation was divided into two significant steps. The first part of the code validation is focused on the mathematical model describing an effect of the magnetic field on the electrically conducting fluids. The second part was dealing with the flow solver itself. The flow solver was validated by various test cases such as unsteady laminar flows in the channel, the Stokes flow in the cylindrical infinite-length containers etc. These tests confirmed the second-order accuracy in space and time.

How the code can capture an onset of the flow stability was presented in [3]. Briefly, the results obtained were in good agreement with the results based on high-order computational methods [2]. The mathematical model for the magnetic force calculation was examined on the cylindrical finite-length container exposed by a rotating magnetic field. Considering the low frequency/induction RMF condition and the cylindrical container, the current density and electrical potential can be derived analytically and taking a form
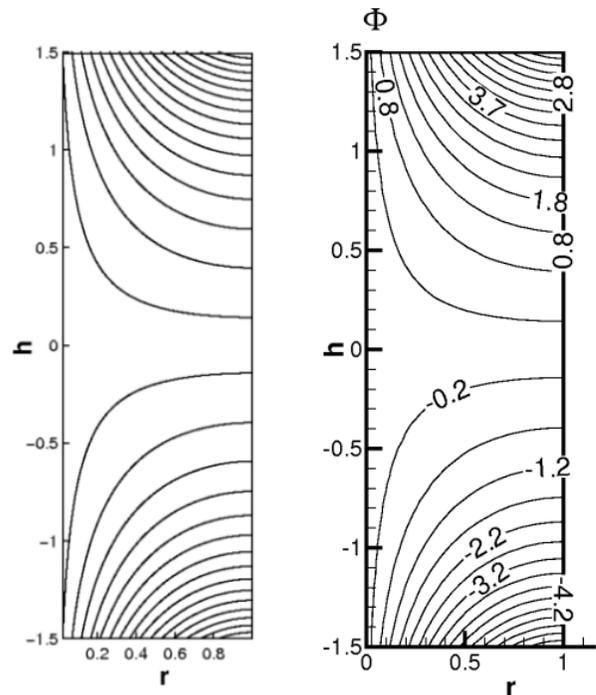

Fig.2 contours of the electric potential calculated by the analytical form (left) and using the mathematical model (right)

Figure 2 shows a good agreement of the electric potential distribution calculated based on the analytical expression by Equation (13) and (12).
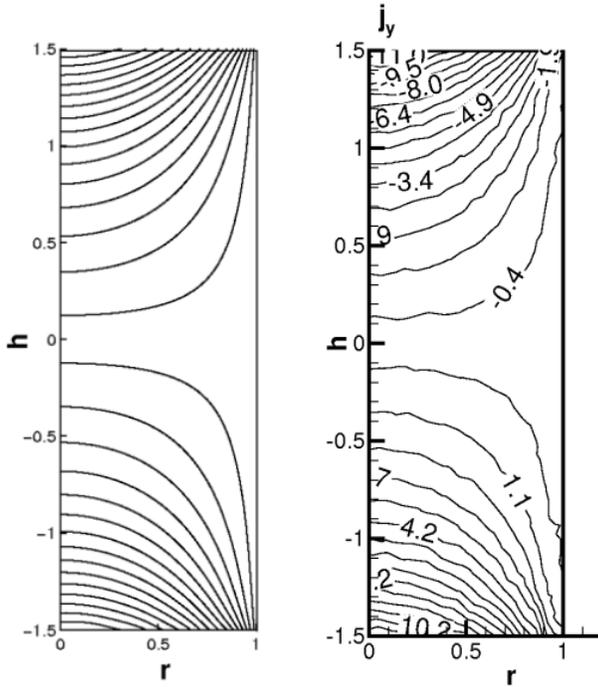
Fig. 3 contours of the y-component of the current density field calculated analytically (left) and using the mathematical model (right) and depicted in the yz- slice

Figure 2 shows a good agreement of the electric potential distribution calculated based on the analytical expression and by Equation (12).
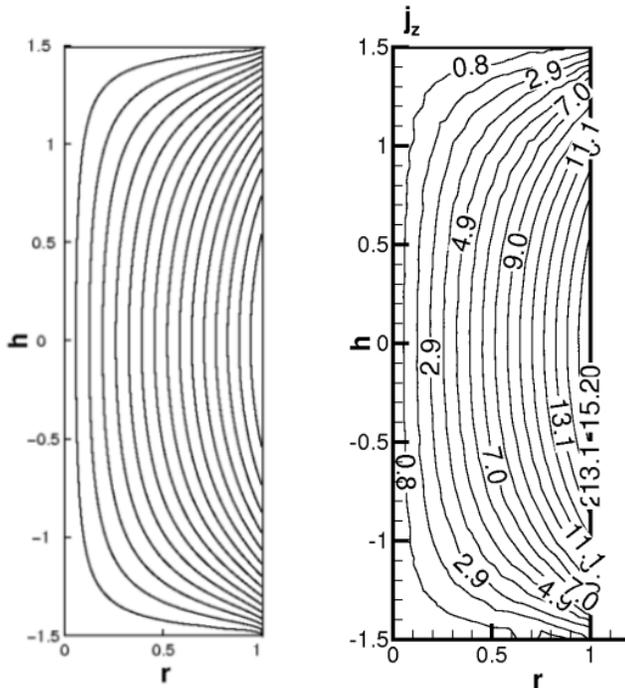

Fig. 4 contours of the z-component of the current density field calculated analytically (left) and using the mathematical model (right) depicted in the yz-slice

Analogous to the electrical potential, Figure 3 and 4 show good agreement of the calculated y- and z-components of the time-depending current density field compared with the analytical solution both in the yz-slice and at the same time position. Because of the symmetry of the magnetic body force distribution in the azimuthal direction, the comparison in the x-component of the magnetic force in the xz-slice will be a qualitatively equivalent. The current density field is essential for the determination of the magnetic force calculation as demonstrated in Equation 5.

V. RESULTS

In order to demonstrate the practical applicability of the computational code for magnetically driven flows, two characteristic examples are chosen: the flow driven by the rotating magnetic field in an axisymmetric and non-axisymetric cavity respectively. In both cases, the Taylor number Ta=1x10^4 is considered.

A. Magnetic force distributions of RMF

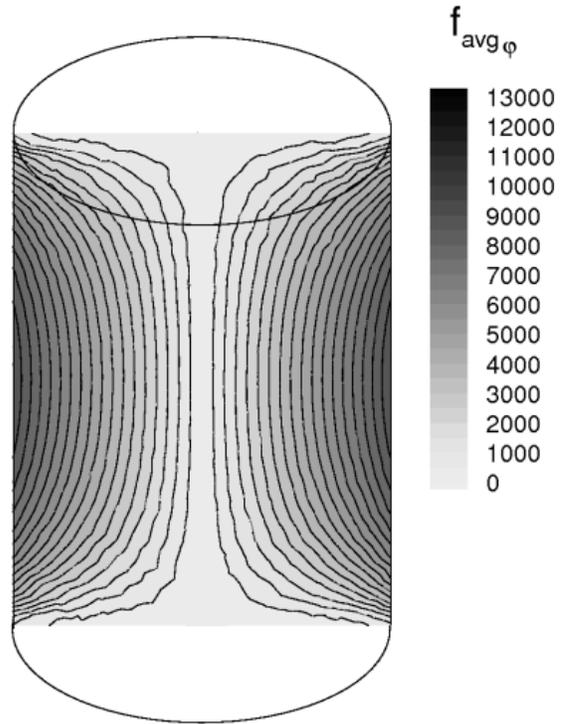The influence of the type of the container on the magnetic force field is demonstrated in Figures 5 and 6.

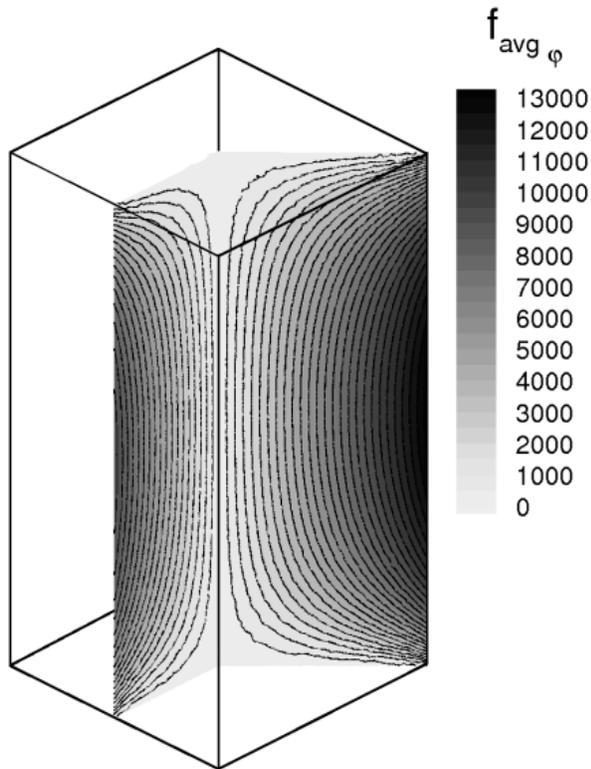Fig. 5 contours of the Lorentz force in a axisymmetric cavity

Fig. 6 contours of the Lorentz force in the square container.

Fig. 7 magnetically driven flows in the cylindrical container

In both containers, the maxima of the intensity of the magnetic body force are close to the vertical walls and the contours of the magnetic force distributions look similar. However, as is expected by the magnetic force definition, the intensity of the Lorentz force is higher at the corner of the square container (non-axisymmetric cavity).

B. *The flow driven by the RMF in an axisymmetric cavity*

The RMF generates a main rotating flow in the azimuthal direction and due to the imbalance between the magnetic forces and pressure; a weak secondary flow appears in the vertical direction [5].

Figure 7 and 8 show the main rotating flow in different horizontal slices irregularly extracted along the z-direction and in the vertical slice, respectively. At $Ta=1 \times 10^4$, the velocity field is axisymetricaly and homogenously distributed. Up to the threshold of the critical Taylor number, the magnetically driven flow remains homogenous and axisymetric [2].

To find more about magnetically driven flows in the transitional or turbulent flow regime, we address to our older publications [5] and [3].
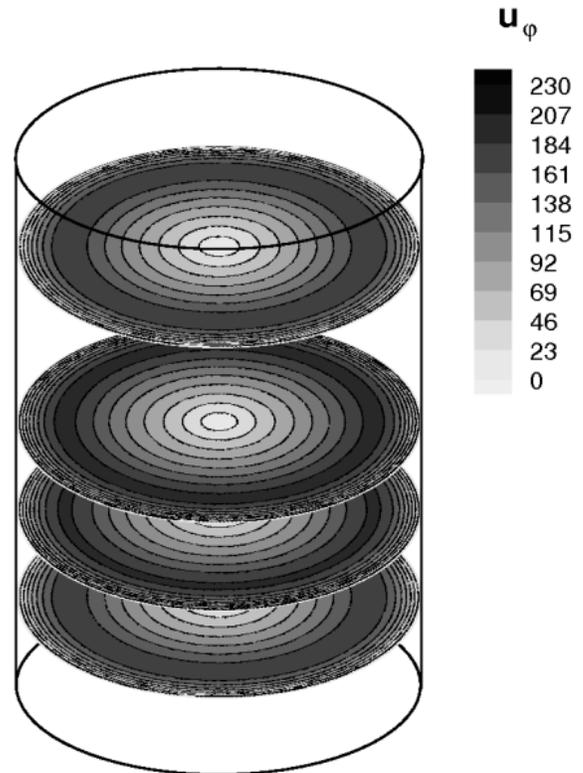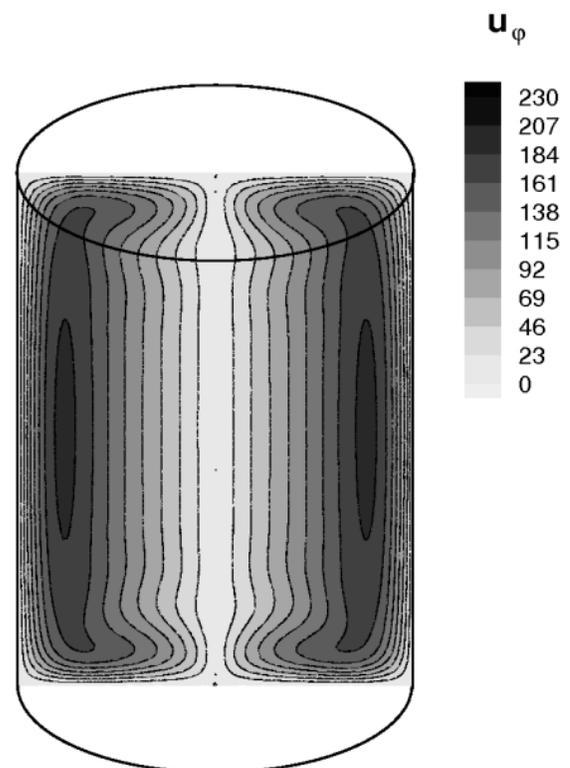

Fig. 8 contours of the rotating flow in the cylindrical cavity

C. The flow driven by the RMF in a non-axisymmetric cavity

While the wide range of various flow studies have been carried out in the last decades in the field of the magnetically driven flow in the cylindrical container, other shape of containers especially non-axisymmetric geometries stayed behind. Consequently, further work will be focused on the flow in the non-axisymmetrical geometry.
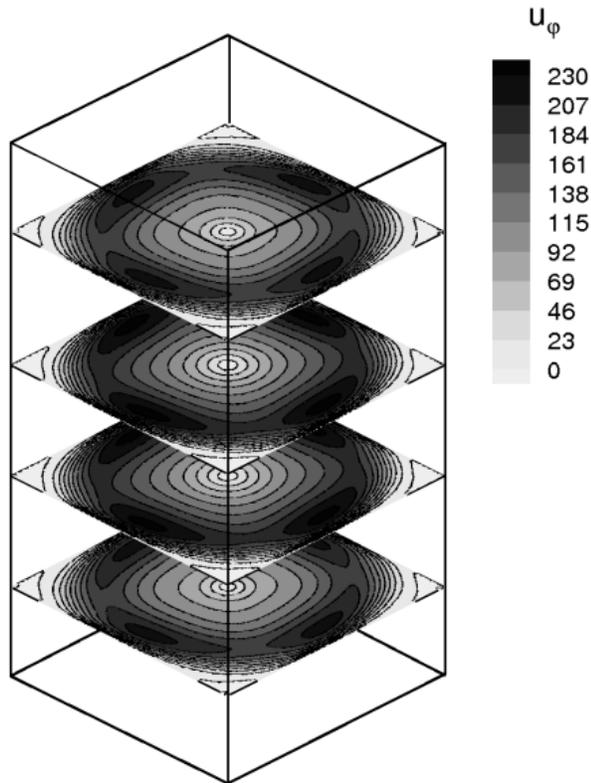

Fig. 9 contours of the rotating flow at horizontal slices in the square container

In general, using the finite-element code presented above, the time-averaged field of the magnetic force can be effectively calculated for any shape of the container. Figures 9 and 10 depict the main rotating flow insight the square container. Obviously the contours of the velocity field are similar to the ones found in the cylindrical container, however, slight differences between both container shapes have been recognized revealing the significant impact of the non-axisymmetrical geometry on the resulting flows.

To find more about this and other effects of the non-axisymetrical geometry of the feature of the magnetically driven flows we address to [6].
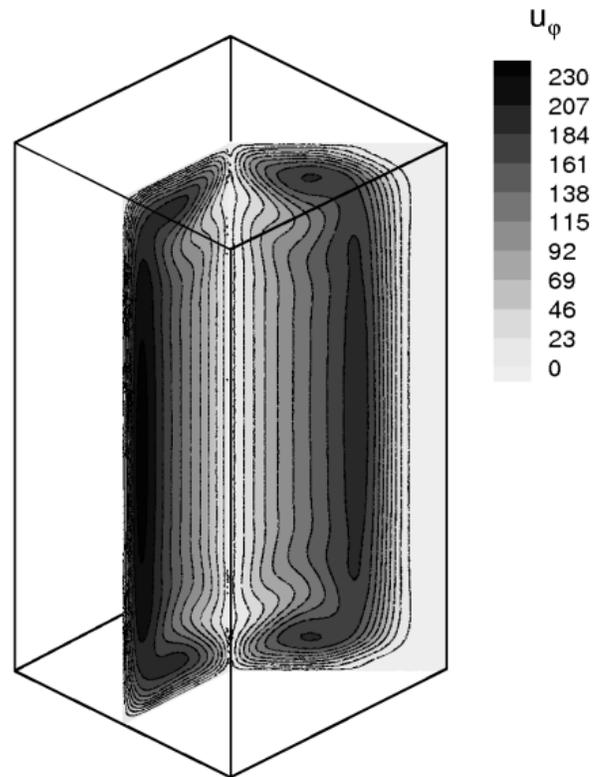

Fig. 10 contours of the rotating flow at the vertical slice in the square container

VI. CONCLUSION

A computational code based on the finite-element method designed especially for the magnetically driven flows was presented. The mathematical model consisted of the Navier-Stokes equations, continuity equation and equations for the calculation of the magnetic field. It was discretized using the Finite-Element Method with SUPG and PSPG stabilization techniques. These numerical approaches were validated on the number of various test cases e.g. the cylindrical container, where time-independent magnetic forces, electric current and electric potential can be derived analytically. The practical application of the computational code was presented on the problem of the RMF in two different containers, in the axisymmetric and non-axisymmetric cavity. The significant influence of both the different containers on the magnetic force distribution as well as magnetically driven flows was discussed briefly.

REFERENCES

[1] G. Karypis and V. Kumar, "ultilevel Algorithms for Multi-Constraint Graph Partitioning," Univ. Minnesota, Dep. Computer Science, TR 98-019, 1998.

[2] I. Grants and G. Gerbeth, "Linear three-dimensional instability of a magnetically driven rotating flow," *J. Fluid Mech*. 463, 2002, pp. 229-239.

[3] J. Stiller, K. Fraňa and A.Cramer, "Transitional and weak turbulent flow in a rotating magnetic field," *Physics of Fluids* 19, 2006, 074105.

[4] J. Stiller and W.E.Nagel, "MG - A Toolbox for Parallel Grid Adaptation and Implementing Unstructured Multigrid Solvers." In: E.H. D'Hollander et al. (Eds.): *Parallel Computing. Fundamentals and Application*, Imperial College Press, 2000.

[5] K. Fraňa, J. Stiller and R.Grundmann, "Transitional and turbulent flows driven by a rotating magnetic field," *Magnetohydrodynamics* 42, 2-3, 2006, pp.187--197.

[6] K.Fraňa, J.Stiller, "A numerical study of flows driven by a rotating magnetic field in a square container," *European Journal of Mechanics / Fluids B* (2007), doi:10.1016/j.euromechflu.2007.10.001

[7] L.Martin Witkowski and J.S.Walker, "Nonaxisymmetric flow in a finite-length cylinder with a rotating magnetic field," *Physics of Fluids* 11, 1999, pp.1821--1826.

[8] P.A. Davidson and J.C.R. Hunt, "Swirling recirculating flow in a liquid-metal column generated by a rotating magnetic field," *J. Fluid Mech*. 185, 1987, pp.67--106.

[9] P.A. Nikrityuk, K. Eckert and R. Grundmann, "Numerical study of a laminar melt flow driven by a rotating magnetic field in enclosed cylinders with different aspect ratios," *Acta Mechanica* 186, 2006, pp.17-35.

[10] S. Yesilyurt, S. Motakel, R. Grugel, and K. Mazuruk, "The effect of the traveling magnetic field (TMF) on the buoyancy-induced convection in the vertical Bridgman growth of semiconductors", J. Cryst. Growth (2004), 263, pp.80-89.

[11] T.E. Tezduyar, S. Mittal, S.E. Ray and R. Shih, "Incompressible flow computations with stabilized bilinear and linear equal-order-interpolation velocity-pressure elements," *Comput. Meth. Appl. Mech. Eng.* 95, 1992, pp.211--242.

[12] T.E. Tezduyar and Y. Osawa, "Finite element stabilization parameters computed from element matrices and vectors," *Comput. Meth. Appl. Mech. Eng.* 190, 2001, pp.411-430.

[13] Yu.M. Gelfgat and J. Priede, "MHD flows on a rotating magnetic field (A review)," *Magnetohydrodynamics* 31, 1-2, 1995, pp.188-200.

K. Fraňa, born in Liberec, Czech Republic in 1975. He received M.S. degree in 1999, Ph.D. degree in 2004 both at the Technical University in Liberec, Department of Power Engineering Equipment. He has received the position Assoc. Prof. at the same university since 2007.

He worked as researcher at the Dresden University of Technology, Institute of Aerospace Engineering, in Germany from 2000 to 2005. He is an author of 5 papers in refereed journals (e.g. Phys. of Fluids, European Journal of Mechanic/Fluid B, Journal of Visualization etc.) and more than 16 papers in conference proceeding. His research interests are in the Finite Element Method and its application to CFD simulations, turbulent flows, modeling and simulation in magnetohydrodynamics.

Assoc. Prof. K. Fraňa, was leader of 2 national research projects and 1 European project. He was a guest at the TU Dresden in the frame of the SFB project 609 and at the University in Vienna, Austria.